Journal of Organometallic Chemistry 882 (2019) 42–49

Contents lists available at ScienceDirect

Journal of Organometallic Chemistry

journal homepage: www.elsevier.com/locate/jorganchem

Desulfination versus decarboxylation as a means of generating three- and five-coordinate organopalladium complexes $[(phen)_nPd(C_6H_5)]^+$ (n = 1 and 2) to study their fundamental bimolecular reactivity

Zilin Wang [a], Yang Yang [a], Paul S. Donnelly [a], Allan J. Canty [b], Richard A.J. O'Hair [a, *]

[a] School of Chemistry, Bio21 Institute of Molecular Science and Biotechnology, The University of Melbourne, Victoria, 3010, Australia
[b] School of Natural Sciences - Chemistry, University of Tasmania, Private Bag 75, Hobart, Tasmania, 7001, Australia

ARTICLE INFO

Article history:
Received 2 October 2018
Received in revised form
21 November 2018
Accepted 21 November 2018
Available online 22 November 2018

Dedicated to Professor Richard Puddephatt on the occasion of his 75th birthday and in recognition of his many important contributions to the activation and transformation of small molecules by platinum group metal complexes.

Keywords:
Decarboxylation
Desulfination
Organopalladium
Electrospray ionization
Mechanism
DFT calculation

ABSTRACT

Routes to the formation of the 1,10-phenanthroline (phen) ligated organopalladium complexes $[(phen)Pd(C_6H_5)]^+$ and $[(phen)_2Pd(C_6H_5)]^+$ via thermal extrusion of CO_2 or SO_2 from mono-nuclear, mono-carboxylate or sulfinate complexes $[(phen)_nPd(O_2XC_6H_5)]^+$ (X = C or S; n = 1 and 2) are examined using a combination of low energy collision induced dissociation experiments in an ion trap mass spectrometer and DFT calculations. $[(phen)Pd(C_6H_5)]^+$ is formed from both $[(phen)Pd(O_2CC_6H_5)]^+$ and $[(phen)Pd(O_2SC_6H_5)]^+$, but only $[(phen)_2Pd(O_2SC_6H_5)]^+$ fragments to form $[(phen)_2Pd(C_6H_5)]^+$. In contrast, $[(phen)_2Pd(O_2CC_6H_5)]^+$ fragments via loss of a phen ligand to form $[(phen)Pd(O_2CC_6H_5)]^+$. The experimental results are consistent with DFT calculations, which show that the barriers associated with the desulfination reactions are lower than those for the decarboxylation reactions. Of the organopalladium cations $[(phen)Pd(C_6H_5)]^+$ and $[(phen)_2Pd(C_6H_5)]^+$, only the three-coordinate complex reacts with pyridine via a ligand coordination reaction to yield $[(phen)Pd(C_6H_5)(NC_5H_5)]^+$ and with formic acid via an acid-base reaction to form $[(phen)Pd(O_2CH)]^+$. DFT calculations highlight that the former reaction energy is −48 kcal/mol while the later reaction proceeds via a favourable six-centered transition structure.

1. Introduction

Modern synthetic chemistry employs transition metal complexes to activate various organic compounds to promote or catalyze chemical bond formation. Palladium-catalyzed cross-coupling reactions, which form C–X bonds (X = C, N, O, S etc.), have revolutionized synthetic chemistry [1]. The last decade has seen intense research activity in developing synthetic transformations involving decarboxylation [2] and desulfination [3]. Most of these studies have focussed on discovering variants of C–C bond coupling reactions such as the Mizoroki-Heck and Suzuki-Miyaura (Scheme 1, eq. 1) reactions [1], in which the C–X bond activation step catalytically generates an organometallic intermediate (Scheme 1, eq. (2)) that then undergoes C–C bond coupling (Scheme 1, eq. 3). The benefit of these new approaches is in terms of atom economy since they replace the use of stoichiometric organometallic reagents (i.e. $R^1B(OH)_2$ in Scheme 1).

In gas-phase studies, we have demonstrated that a wide range of metal carboxylates can be decarboxylated to form the crucial organometallic intermediate [6]. Coinage metal sulfinates are more readily desulfinated than coinage metal carboxylates are decarboxylated [7]. Nitrogen based ligands have a rich history in group 10 organometallic chemistry, having been pioneered by Richard Puddephatt and others [8]. We and others have been using 1,10-phenanthroline (phen) in both Pd mediated decarboxylation [9,10] and desulfination reactions [11]. Apart from a single study that employed DFT calculations to compare the energetics of decarboxylation versus desulfination [11a], little is known about their fundamental fragmentation reactions. Here we use multistage mass spectrometry (MS^n) experiments and DFT calculations to:

* Corresponding author.
E-mail address: rohair@unimelb.edu.au (R.A.J. O'Hair).

https://doi.org/10.1016/j.jorganchem.2018.11.028
0022-328X/

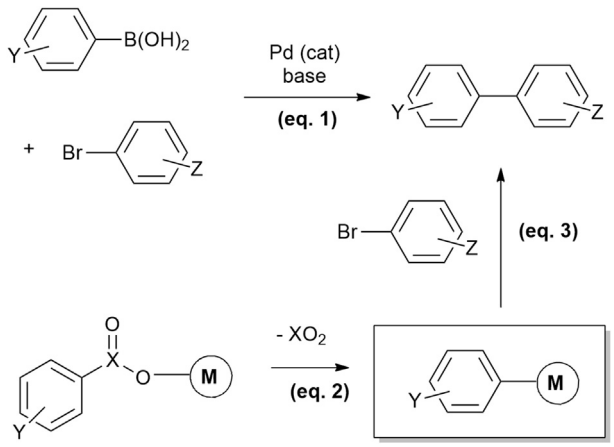

Scheme 1. Suzuki-Miyaura reaction (eq. 1) and related variants involving decarboxylation (X = C) [4] or desulfination (X = S) [5] to form organometallic intermediates (eq. 2), which then undergo C–C bond coupling (eq. 3).

examine the unimolecular fragmentation reactions of mononuclear mono-carboxylate or sulfinate complexes $[(phen)_nPd(O_2XC_6H_5)]^+$ (X = C or S; n = 1 and 2); and compare the bimolecular reactions of the resultant organometallic cations $[(phen)_2Pd(C_6H_5)]^+$ and $[(phen)Pd(C_6H_5)]^+$ with pyridine to examine ligand addition [12] or substitution reactions [13] and formic acid to examine protonation of the phenyl group to liberate benzene [14].

2. Materials and methods

2.1. Materials

1,10-phenanthroline (phen), $Pd(O_2CCF_3)_2$, $PhSO_2Na$, benzoic acid, formic acid and pyridine were obtained from Sigma Aldrich (reagent grade). All solvents were HPLC grade. All purchased materials were used without further purification.

2.2. Sample preparation for mass spectrometry experiments

The gas phase collision-induced dissociation (CID) of $[(phen)_nPd(O_2XC_6H_5)]^+$ (X = C or S; n = 1 and 2) to form $[(phen)_2Pd(C_6H_5)]^+$ or $[(phen)Pd(O_2XC_6H_5)]^+$ to form $[(phen)Pd(C_6H_5)]^+$ and subsequent ion-molecule reaction (IMR) studies with formic acid and pyridine were conducted in a similar method to those reported for the reactivity studies of $[(phen)Pd(R)]^+$ complexes [9]. Briefly, methanolic solutions (10 μL) of palladium trifluoroacetate (10 mM), sodium benzene sulfinate (10 mM) and 1,10-phenanthroline (phen) (10 mM) were mixed and then diluted to a final concentration of Pd of 0.05 mM.

2.3. Mass spectrometry experiments

The solutions prepared as described above were transferred via a syringe pump operating at 5 μL min^{-1} to the electrospray ionization source of a Thermo Finnigan LTQ ESI mass spectrometer previously modified to allow for the introduction of neutral reagents into the ion trap [15,16]. Data was collected with three microscans and are the average of 20–100 spectra.

2.4. Ion-molecule reaction experiments

All IMR rate measurements were conducted by isolating the reactant ion $[(phen)_nPd(C_6H_5)]^+$ (n = 1, 2) in an MS^3 experiment and then allowing it to react with formic acid or pyridine. Single isotope peaks were used, and each reaction measurement was taken on a separate day. The mass selection windows and scan mass range were kept constant throughout. Ion-molecule collision rates were calculated with the program COLRATE using the average dipole orientation (ADO) theory of Su and Bowers [17].

2.5. Mass spectrometry source condition

Typical electrospray source conditions were:

2.5.1. CID

Sheath Gas = 10 arbitrary units, Auxiliary Gas = 5 arbitrary units, Sweep Gas = 0 arbitrary units, Spray Voltage = 4 kV, Capillary Temp. = 250 °C, Capillary Voltage = 2 V, Tube Lens Voltage = 75 V. The precursor ion was mass selected with a window of 1 *m/z* and collision induced dissociation was carried out using the helium bath gas by activating the ion with an activation time of 30 ms. A normalized collision energy (NCE) was chosen to deplete the precursor ion to 10%.

2.5.2. IMR

Sheath Gas = 10 arbitrary units, Auxiliary Gas = 5 arbitrary units, Sweep Gas = 0 arbitrary units, Spray Voltage = 4 kV, Capillary Temp. = 250 °C, Capillary Voltage = 2 V, Tube Lens Voltage = 75 V.

2.6. Theoretical calculations

Geometry optimizations and electronic energy calculations were performed using the Gaussian 09 molecular modelling package [18a] to provide insights into the desulfination of $[(phen)_nPd(O_2SC_6H_5)]^+$, decarboxylation of $[(phen)_nPd(O_2CC_6H_5)]^+$ and reactions of the organometallic palladium complexes $[(phen)_nPd(C_6H_5)]^+$ with formic acid and pyridine. Structures of minima and transition states were optimized using the M06 functional [19]. The Stuttgart Dresden (SDD) basis set and effective core potential were used for the palladium atom [20], while the 6-31 + G(d) all-electron basis set was used for carbon, nitrogen, oxygen, sulfur and hydrogen [21] – this basis set is designated as BS1. Frequency calculations were carried out at the same level of theory as those for the structural optimization. Transition structures were located using the Berny algorithm. Intrinsic reaction coordination (IRC) calculations were used to confirm the connectivity between transition structures and minima. Only singlet calculations have been carried out since calculations on related ligated palladium cations have shown that these are considerably more stable than triplets [22].

To further refine the energies obtained from the M06/6-31 + G(d)/SDD calculations, we carried out a series of single-point energy calculations for all of the structures using different methods in conjunction with the larger basis set utilizing def2-tzvp for all atoms along with the effective core potential including scalar relativistic effects for Pd [23], which is designated as BS2. The different DFT methods used include: the Minnesota functionals M06 [19] and MN15 [24]; wB97XD [25]; and the dispersion corrected Becke functionals B3LYP-D3BJ and CAM-B3LYP-D3BJ [26]. The resultant energies are corrected for zero point energies and the relative reaction energies for the various methods can be compared in Table S1.

To estimate the corresponding enthalpy, ΔH, and Gibbs energies, ΔG, the corrections were calculated at the M06/6-31 + G(d)/SDD levels at both STP conditions and at the T (298 K) and P (2 mtorr) conditions of the ion trap mass spectrometer [16] and finally added to the corresponding single-point energies. Tables S2 and S3

compare the reaction enthalpies and free energies respectively using the various DFT methods.

We have used the relative reaction energies obtained from the CAM-B3LYP-D3BJ/BS2/M06/BS1 calculations throughout since this combination of basis set and method performs best when comparing the types of competing fragmentation reactions observed for $[(phen)_2Pd(O_2SC_6H_5)]^+$ and $[(phen)_2Pd(O_2CC_6H_5)]^+$. We use relative energies rather than enthalpies or Gibbs free energies for the following reasons: (1) under the low energy CID conditions used, the ions undergo multiple collisions with the helium bath gas resulting in slow "heating" until fragmentation occurs [27]. Thus the effective temperature is unknown and will vary for different systems. (2) Under IMR conditions Dau et al. have recently highlighted that the reaction energy rather than the Gibbs free energy is the relevant thermodynamic parameter to use for low-pressure bimolecular reactions [28].

All optimized structures reported here were subjected to vibrational frequency analysis to ensure they corresponded to true minima (no imaginary frequency) or transition states (one imaginary frequency). The Supplementary Information file contains GaussView [18b] 3D molecular structures of all species together with the Cartesian coordinates.

3. Results and discussions

3.1. Experimental and DFT calculations on the formation of the organometallic ions $[(phen)_nPd(C_6H_5)]^+$ (n = 1 and 2) via decarboxylation or desulfination

Positive ion electrospray ionization of methanolic solutions of mixtures of 1,10-phenanthroline (phen), palladium trifluoroacetate, and either benzoic acid or sodium benzene sulfinate gave a range of cations including the mono-nuclear mono-carboxylate or sulfinate complexes $[(phen)_nPd(O_2XC_6H_5)]^+$ (X = C or S; n = 1 and 2), which were mass-selected and subjected to collision-induced dissociation (CID).

3.1.1. Formation of $[(phen)Pd(C_6H_5)]^+$

As reported previously, CID of $[(phen)Pd(O_2CC_6H_5)]^+$ cleanly generates $[(phen)Pd(C_6H_5)]^+$ (eq. (4), X = C) [9e]. CID of $[(phen)Pd(O_2SC_6H_5)]^+$ also cleanly generates $[(phen)Pd(C_6H_5)]^+$ (eq. (4), X = S) (Fig. S1). The DFT calculated potential energy diagram for both types of extrusion reactions are similar. Since that for $[(phen)Pd(O_2CC_6H_5)]^+$ has been previously reported at a slightly different level of theory [9e], the potential energy diagram for $[(phen)Pd(O_2SC_6H_5)]^+$ is shown in Fig. 1. Desulfination is initiated by **TS1b-2b**, which isomerizes the four-coordinate sulfinate complex **1b** to the reactive three-coordinate complex, **2b**, which then readily desulfinates via the four-centered **TS2b-3b**, to give the organometallic complex **3b** in which the SO_2 is bound to the Pd center via an O atom. The isomeric complex **3b'** in which the SO_2 is bound to the Pd center via an S atom has a similar stability. The final step involves loss of SO_2 to give the three-coordinate complex, **4a**. **TS1b-2b** is the rate determining step.

$$[(phen)Pd(O_2XC_6H_5)]^+ \rightarrow [(phen)Pd(C_6H_5)]^+ + XO_2 \quad (4)$$

The DFT calculated potential energy diagram for $[(phen)Pd(O_2CC_6H_5)]^+$ at the same level of theory is given in Fig. S2. The rate determining step for decarboxylation, **TS1a-2a**, is that which isomerizes the four-coordinate carboxylate complex **1a** to the reactive three-coordinate complex, **2a**. Complex **2a** then decarboxylates via the four-centered **TS2a-3a**, to give the organometallic complex **3a** in which the CO_2 is bound to the Pd center via an O atom, which then loses CO_2 to form **4a**. The barrier for the rate determining desulfination step is lower than that for decarboxylation by about 16 kcal/mol, consistent with DFT studies on related palladium complexes [11a] and with previous gas-phase studies that have shown coinage metal complexes more readily undergo desulfination [7]. Varying the DFT methods does not have a major effect on the reaction energies (Table S1), with **TS1b-2b** and **TS1a-2a** remaining the rate determining steps for desulfination and decarboxylation respectively. The trends for ΔH (Table S2) follow those for ΔE. There are significant differences when comparing the overall reaction energetics ΔE (or ΔH) to those of ΔG (Table S3). This is due to the fact that during CID one particle is transformed into two particles which has a favourable entropic effect.

3.1.2. Formation of $[(phen)_2Pd(C_6H_5)]^+$

The CID spectra of $[(phen)_2Pd(O_2XC_6H_5)]^+$ (Fig. 2) are more diverse in their reaction chemistry than those for $[(phen)Pd(O_2XC_6H_5)]^+$. The complex with two coordinated phenanthroline ligands, $[(phen)_2Pd(O_2CC_6H_5)]^+$, does not undergo decarboxylation (eq. (4), X = C), instead it exclusively loses phen to give [(phen)

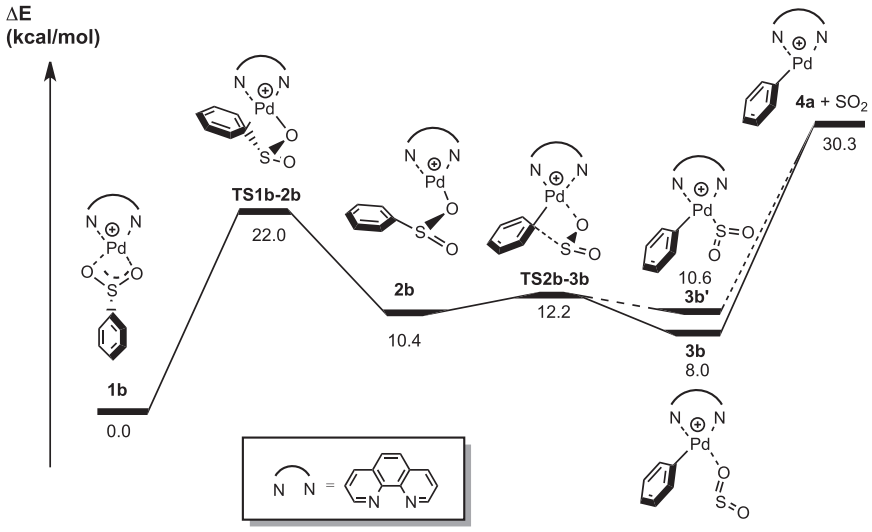

Fig. 1. Results of DFT calculations on desulfination of $[(phen)Pd(O_2SC_6H_5)]^+$, **1b** at the CAM-B3LYP-D3BJ/BS2//M06/BS1 level of theory. Relative energies are in kcal/mol.

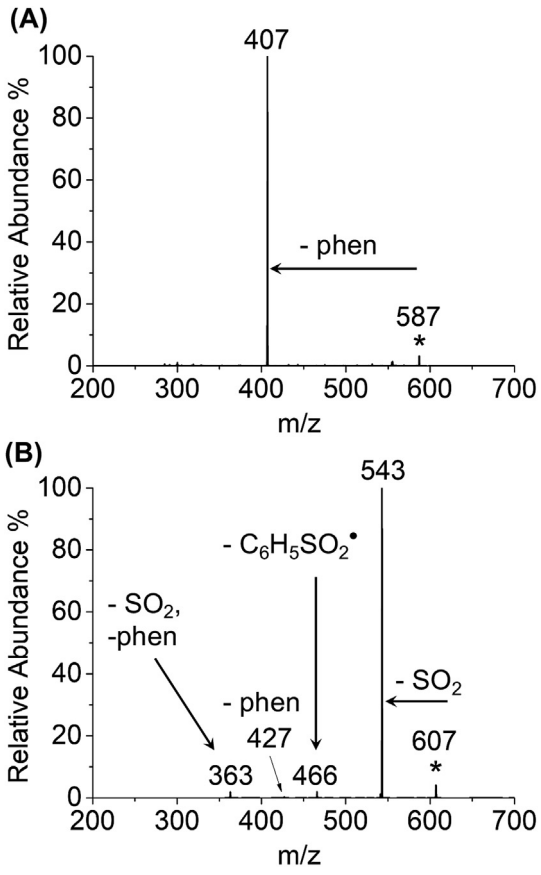

Fig. 2. CID of mass selected complexes: (a) $[(phen)_2Pd(O_2CC_6H_5)]^+$ ($m/z = 587$, 15 NCE); (b) $[(phen)_2Pd(O_2SC_6H_5)]^+$ ($m/z = 607$, 13 NCE). The mass-selected precursor ions are denoted by asterisks.

$Pd(O_2CC_6H_5)]^+$ (eq. (6)). In contrast, the dominant fragmentation pathway for $[(phen)_2Pd(O_2SC_6H_5)]^+$ is desulfination to give the organometallic complex $[(phen)_2Pd(C_6H_5)]^+$ (eq. (5), X = S). Only a few related five-coordinate $[(phen)_2Pd(R)]^+$ complexes have been synthesized and structurally characterized via X-ray crystallography, including: R = CH_3; O_2NCH_2; and $CH_3OC(O)$ [29]. Other minor fragmentation pathways observed for $[(phen)_2Pd(O_2SC_6H_5)]^+$ include loss of phen to give $[(phen)Pd(O_2SC_6H_5)]^+$ (eq. (6), X = S) and Pd–O bond homolysis via $C_6H_5XO_2$ loss to yield the presumably formally Pd(I) cation, $[(phen)_2Pd]^{+\cdot}$ (eq. (7), X = S). The related Ni(I) cation, $[(phen)_2Ni]^{+\cdot}$ has recently been prepared in the gas-phase via reduction of $[(phen)_2Ni]^{2+}$ in ion-ion reactions [30]. The ion $[(phen)Pd(C_6H_5)]^+$ arises from secondary fragmentation reactions of $[(phen)Pd(O_2SC_6H_5)]^+$ (Fig. S1).

$$[(phen)_2Pd(O_2XC_6H_5)]^+ \rightarrow [(phen)_2Pd(C_6H_5)]^+ + XO_2 \quad (5)$$

$$\rightarrow [(phen)Pd(O_2XC_6H_5)]^+ + phen \quad (6)$$

$$\rightarrow [(phen)_2Pd]^{+\cdot} + C_6H_5XO_2^{\cdot} \quad (7)$$

The energetics for all three pathways are compared for $[(phen)_2Pd(O_2CC_6H_5)]^+$, **5a** (Fig. 3) and for $[(phen)_2Pd(O_2SC_6H_5)]^+$ (**5b** in Fig. 4) to probe why only phen loss is observed for $[(phen)_2Pd(O_2CC_6H_5)]^+$ while desulfination is in competition with both phen loss and bond homolysis for $[(phen)_2Pd(O_2SC_6H_5)]^+$.

Unlike the $[(phen)Pd(O_2XC_6H_5)]^+$ complexes in which the carboxylate or sulfinate ligands bind in a bidentate fashion, in both **5a** and **5b** these ligands bind in a monodentate fashion due to the presence of the additional bidentate phen ligand. In the case of **5a**, the energetics associated with the loss of the phen ligand (eq. (6)) are found to be substantially less than those for decarboxylation (eq. (5)) or bond homolyses (eq. (7)), in agreement with the

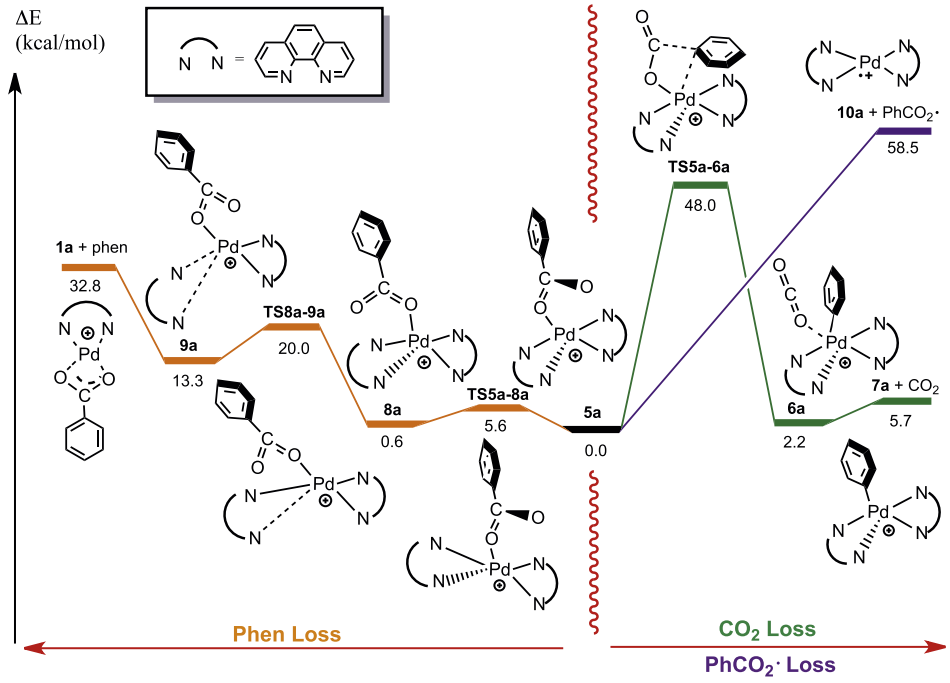

Fig. 3. Results of DFT calculations on the competition between decarboxylation and phen loss of $[(phen)_2Pd(O_2CC_6H_5)]^+$, **5a** at the CAM-B3LYP-D3BJ/BS2//M06/BS1 level of theory. Relative energies are in kcal/mol.

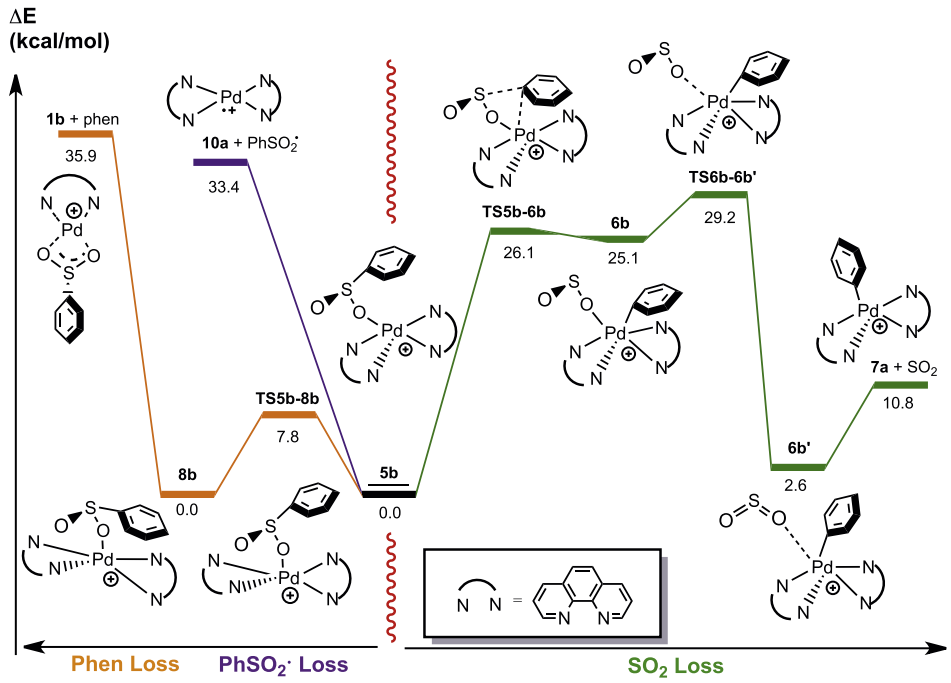

Fig. 4. Results of DFT calculations on the competition between desulfination and phen loss of $[(phen)_2PdO_2SC_6H_5]^+$, **5b** at the CAM-B3LYP-D3BJ/BS2//M06/BS1 level of theory. Relative energies are in kcal/mol.

experiments, where phen loss is the only one of these reactions observed (Fig. 2a). Decarboxylation proceeds via a single four-centered transition structure **TS5a-6a**, while the key transition structure for phen loss is **TS8a-9a**. Under the slow "heating" conditions used in the ion trap, fragmentation occurs under kinetic rather than thermodynamic control. Thus when competing fragmenting reactions are being considered, it is important to consider the energies of the highest species along each of the different reaction coordinates. In the case of the three potentially competing fragmentation pathways for $[(phen)_2Pd(O_2CC_6H_5)]^+$ (Fig. 3) the overall energy for phen loss at 32.8 kcal/mol is less that **TS5a-6a** (+48 kcal/mol) for decarboxylation and the overall energy for $C_6H_5CO_2$ loss (58.5 kcal/mol). This is consistent with the experiments, where only phen loss is observed.

The change in experimentally preferred fragmentation channel on moving from $[(phen)Pd(O_2CC_6H_5)]^+$ **5a** to $[(phen)Pd(O_2SC_6H_5)]^+$ **5b** is consistent with the differences in energetics for all three fragmentation channels shown in Figs. 3 and 4. The rate determining transition state for desulfination, **TS6b-6b'**, lies about 19 kcal/mol below the rate determining transition state for decarboxylation, **TS5a-6a**. The energy for bond homolyses also drops by around 25 kcal/mol, consistent with this channel now being experimentally observed for $[(phen)Pd(O_2SC_6H_5)]^+$ (Fig. 2b). In contrast, the energy for phen loss increases by 3 kcal/mol consistent with this channel now becoming a minor pathway for $[(phen)Pd(O_2SC_6H_5)]^+$. Overall the key energies associated with the different reaction coordinates are: desulfination **TS6b-6b'** (29.2 kcal/mol) < $C_6H_5SO_2$ loss (33.4 kcal/mol) < phen loss (35.9). This is consistent with desulfination being the dominant reaction while $C_6H_5SO_2$ loss is a minor pathway and phen loss is even smaller (Fig. 2B).

Once again, varying the DFT method does not have a major effect on the reaction energies (Table S1) and the above discussion regarding ΔE versus ΔH (Table S2) and ΔG (Table S3) holds true for the competing fragmentation reactions for $[(phen)_2Pd(O_2CC_6H_5)]^+$ and $[(phen)_2Pd(O_2SC_6H_5)]^+$.

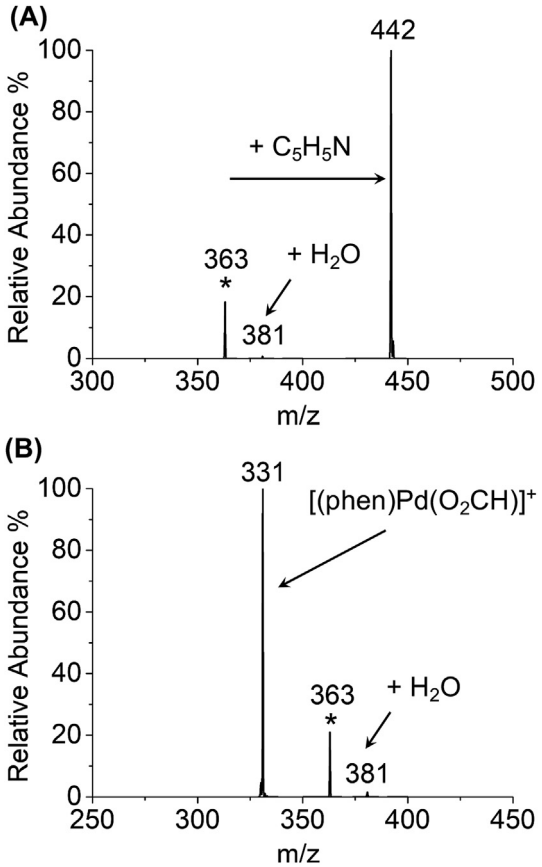

Fig. 5. Ion-molecule reactions of $[(phen)Pd(C_6H_5)]^+$ with: (a) pyridine; (b) formic acid. The mass-selected precursor ions are denoted by asterisks.

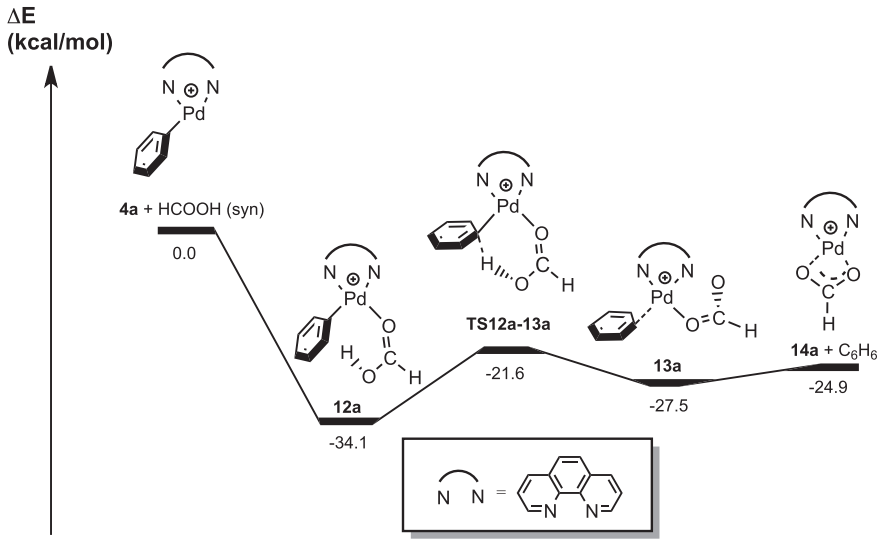

Fig. 6. Results of DFT calculations on the reaction of $[(phen)Pd(C_6H_5)]^+$ with formic acid at the CAM-B3LYP-D3BJ/BS2//M06/BS1 level of theory. Relative energies are in kcal/mol.

3.2. Ion-molecule reactions of three- and five-coordinate organopalladium complexes $[(phen)_nPd(C_6H_5)]^+$ (n = 1 and 2).

The formation of both $[(phen)Pd(C_6H_5)]^+$ and $[(phen)_2Pd(C_6H_5)]^+$ via extrusion reactions provides a unique opportunity to directly compare their gas-phase reactivity. We have chosen two different neutral reagents: pyridine which has previously been used to titrate vacant coordination sites in three-coordinate Pt(II) complexes [10,31], to examine ligand substitution reactions in four-coordinate Pt(II) complexes [11], and formic acid, which has been used to protonate coordinated anionic ligands in metal complexes [12].

Mass spectra resulting from the ion-molecule reactions of $[(phen)Pd(C_6H_5)]^+$ (Fig. 5), reveal a minor peak at *m/z* 381 resulting from addition of adventitious water (eq. (8)), a reaction that has been discussed previously [7b]. The three-coordinate complex $[(phen)Pd(C_6H_5)]^+$ rapidly reacts with pyridine at close to the collision rate (1.1×10^{-9} cm^3 molecules^{-1} s^{-1}, reaction efficiency of 77%) via adduct formation (eq. (9), Fig. 5a). This is consistent with DFT calculations which predict that coordination of pyridine to **4a** has a reaction energy of −48 kcal/mol (Fig. S3). In contrast, the five-coordinate complex $[(phen)_2Pd(C_6H_5)]^+$ is unreactive towards pyridine under the conditions used (eq. (10), data not shown).

$$[(phen)Pd(C_6H_5)]^+ + H_2O \rightarrow [(phen)Pd(C_6H_5)(OH_2)]^+ \quad (8)$$

$$[(phen)Pd(C_6H_5)]^+ + C_5H_5N \rightarrow [(phen)Pd(C_6H_5)(NC_5H_5)]^+ \quad (9)$$

$$[(phen)_2Pd(C_6H_5)]^+ + C_5H_5N \rightarrow \text{no reaction} \quad (10)$$

The three-coordinate complex $[(phen)Pd(C_6H_5)]^+$ rapidly reacts with formic acid (7×10^{-10} cm^3 molecules^{-1} s^{-1}, reaction efficiency of 65%) via an acid-base reaction to give the complex with a coordinated formate (eq. (11), Fig. 5b). $[(phen)_2Pd(C_6H_5)]^+$ does not undergo an acid-base reaction. No new reaction products are observed under the conditions used (eq. (12), data not shown).

$$[(phen)Pd(C_6H_5)]^+ + HCO_2H \rightarrow [(phen)Pd(O_2CH)]^+ + C_6H_6 \quad (11)$$

$$[(phen)_2Pd(C_6H_5)]^+ + HCO_2H \rightarrow \text{no reaction} \quad (12)$$

The potential energy diagram associated with the acid-base reaction of $[(phen)Pd(C_6H_5)]^+$ (Fig. 6) suggest the reaction involves coordination of formic acid through the carbonyl oxygen atom to give complex **12a**, which then traverses the six-centered transition structure **TS12a-13a** to give complex **13a**, which then loses benzene to give the formate complex $[(phen)Pd(O_2CH)]^+$, **14a**. A higher energy pathway involving a four-centered transition structure **TS12a-13a** was also found (Fig. S4). The fact that water only undergoes adduct formation (eq. (8)) whereas formic acid undergoes an acid-base reaction (eq. (11)) is likely due to the higher acidity of formic acid, over 40 kcal/mol in the gas-phase [32], and that for water a four-centered transition structure must be traversed for the acid-base reaction to proceed, whereas for formic acid an energetically more accessible six-centered transition structure is available. Varying the DFT method does not have a major effect on the reaction energies (Table S1). The trends for ΔH (Table S2) follow those for ΔE and there is little difference when comparing ΔH under STP conditions to those of the ion trap mass spectrometer T = 298 K and P = 2 mtorr). As discussed by Dau et al., [27] there are significant differences when comparing ΔE (or ΔH) to those of ΔG (Table S3) under the ion trap mass spectrometer conditions. This is due to the fact that for ion-molecule reactions two particles transform into one particle in the entrance channel resulting in an unfavourable entropic effect.

4. Conclusions

Low energy CID of ligated palladium complexes provides access to a range of reactive intermediates. Extrusion of CO_2 and SO_2 gives the three-coordinate complex $[(phen)Pd(C_6H_5)]^+$. This coordinatively unsaturated complex readily reacts with pyridine to form $[(phen)Pd(C_6H_5)(NC_5H_5)]^+$ and reacts with formic acid in an acid-base reaction to give $[(phen)Pd(O_2CH)]^+$. Mechanistic studies on the use of palladium mediated decarboxylation and desulfination reactions followed by insertion of isocyanates are underway with the aim of developing synthetic protocols for the one pot synthesis of amides.

Acknowledgments

We thank the Australian Research Council for financial support DP180101187 (to RAJO, PSD and AJC). The authors gratefully

acknowledge the generous allocation of computing time from the University of Tasmania and the National Computing Infrastructure (fz2 and zg2). We thank Dr Bun Chen for helpful discussions on benchmarking.

Appendix A. Supplementary data

Supplementary data to this article can be found online at https://doi.org/10.1016/j.jorganchem.2018.11.028.

References

[1] C.C.C. Johansson Seechurn, M.O. Kitching, T.J. Colacot, V. Snieckus, Palladium-catalyzed cross-coupling: a historical contextual perspective to the 2010 Nobel Prize, Angew. Chem. Int. Ed. 51 (2012) 5062–5085.

[2] N. Rodriguez, L.J. Goossen, Decarboxylative coupling reactions: a modern strategy for C–C-bond formation, Chem. Soc. Rev. 40 (2011) 5030–5048.

[3] D.H. Ortgies, A. Hassanpour, F. Chen, S. Woo, P. Forgione, Desulfination as an emerging strategy in palladium-catalyzed C–C coupling reactions, Eur. J. Org Chem. 3 (2016) 408–425.

[4] (a) G. Deng, L.M. Levy, Synthesis of biaryls via catalytic decarboxylative coupling, Science 313 (2006) 662–664;
(b) L.J. Goossen, N. Rodríguez, B. Melzer, C. Linder, G. Deng, L.M. Levy, Biaryl synthesis via Pd-catalyzed decarboxylative coupling of aromatic carboxylates with aryl halides, J. Am. Chem. Soc. 129 (2007) 4824–4833;
(c) O. Baudoin, New approaches for decarboxylative biaryl coupling, Angew. Chem. Int. Ed. 46 (2007) 1373–1375.

[5] (a) D.H. Ortgies, A. Barthelme, S. Aly, B. Desharnais, S. Rioux, P. Forgione, Scope of the desulfinylative palladium-catalyzed cross-coupling of aryl sulfinates with aryl bromides, Synthesis 45 (2013) 694–702;
(b) D.H. Ortgies, P. Forgione, A ligand-free palladium-catalyzed cross-coupling of aryl sulfinates with aryl bromides, Synlett 24 (2013) 1715–1721.

[6] R.A.J. O'Hair, N.J. Rijs, Gas phase studies of the Pesci decarboxylation reaction: synthesis, structure, and unimolecular and bimolecular reactivity of organometallic ions, Acc. Chem. Res. 48 (2015) 329–340.

[7] (a) L.O. Sraj, G.N. Khairallah, G. da Silva, R.A.J. O'Hair, Who wins: Pesci, Peters, or Deacon? Intrinsic reactivity orders for organocuprate formation via ligand decomposition, Organometallics 31 (2012), 1801-1087;
(b) Q. Jin, J. Li, A. Ariafard, A.J. Canty, R.A.J. O'Hair, Substituent effects in the decarboxylation reactions of coordinated arylcarboxylates in dinuclear copper complexes, [(napy) Cu_2 $(O_2CC_6H_4X)]^+$, Eur. J. Mass Spectrom. 23 (2017) 351–358.

[8] (a) N. Chaudhury, M.G. Kekre, R.J. Puddephatt, The reactivity of methylnickel, -palladium, and -platinum compounds towards alkenes and alkynes, J. Organomet. Chem. 73 (1974) C17–C19;
(b) L.M. Rendina, R.J. Puddephatt, Oxidative addition reactions of organoplatinum(II) complexes with nitrogen- donor ligands, Chem. Rev. 97 (1997) 1735–1754;
(c) A. Behnia, M.A. Fard, J.M. Blacquiere, R.J. Puddephatt, Mild and selective Pd-Ar protonolysis and C- H activation promoted by a ligand aryloxide group, Dalton Trans. 47 (2018) 3538–3548;
(d) K.T. Aye, A.J. Canty, M. Crespo, R.J. Puddephatt, J.D. Scott, A.A. Watson, Alkyl halide transfer from palladium(IV) to platinum(II) and a study of reactivity, selectivity, and mechanism in this and related reactions, Organometallics 8 (1989) 1518–1522;
(e) P.K. Byers, A.J. Canty, M. Crespo, R.J. Puddephatt, J.D. Scott, Reactivity and mechanism in oxidative addition to palladium(II) and reductive elimination from palladium(IV) and an estimate of the palladium methyl bond energy, Organometallics 7 (1988) 1363–1367.

[9] (a) M. Woolley, G.N. Khairallah, P.S. Donnelly, R.A.J. O'Hair, Nitrogen adduction by three coordinate group 10 cations: platinum is favoured over nickel and palladium, Rapid Commun. Mass Spectrom. 25 (2011) 2083–2088;
(b) M. Woolley, A. Ariafard, G.N. Khairallah, K.H.Y. Kwan, P.S. Donnelly, J.M. White, A.J. Canty, B.F. Yates, R.A.J. O'Hair, Decarboxylative-coupling of allyl acetate catalyzed by group 10 organometallics,[(phen) M $(CH_3)]^+$, J. Org. Chem. 79 (2014) 12056–12069;
(c) M. Woolley, G.N. Khairallah, G. da Silva, P.S. Donnelly, B.F. Yates, R.A.J. O'Hair, Role of the metal, ligand, and alkyl/aryl group in the hydrolysis reactions of group 10 organometallic cations [(L) M (R)]$^+$, Organometallics 32 (2013) 6931–6944;
(d) M. Woolley, G.N. Khairallah, G. da Silva, P.S. Donnelly, B.F. Yates, R.A.J. O'Hair, Direct versus water-mediated protodecarboxylation of acetic acid catalyzed by group 10 carboxylates, [(phen) M $(O_2CCH_3)]^+$, Organometallics 33 (2014) 5185–5197;
(e) A. Noor, J. Li, G.N. Khairallah, Z. Li, H. Ghari, A.J. Canty, A. Ariafard, P.S. Donnelly, R.A.J. O'Hair, A one-pot route to thioamides discovered by gas-phase studies: palladium-mediated CO_2 extrusion followed by insertion of isothiocyanates, Chem. Commun. 53 (2017) 3854–3857.

[10] (a) F. Svensson, R.S. Mane, J. Sävmarker, M. Larhed, C. Sköld, Theoretical and experimental investigation of palladium(II)-catalyzed decarboxylative addition of arenecarboxylic acid to nitrile, Organometallics 32 (2013) 490–497;
(b) J. Rydfjord, F. Svensson, A. Trejos, P.J.R. Sjöberg, C. Sköld, J. Sävmarker, L.R. Odell, M. Larhed, Decarboxylative palladium(II)-catalyzed synthesis of aryl amidines from aryl carboxylic acids: development and mechanistic investigation, Chem. Eur J. 19 (2013) 13803–13810.

[11] (a) B. Skillinghaug, C. Sköld, J. Rydfjord, F. Svensson, M. Behrends, J. Sävmarker, P.J.R. Sjöberg, M. Larhed, Palladium(II)-catalyzed desulfitative synthesis of aryl ketones from sodium arylsulfinates and nitriles: scope, limitations, and mechanistic studies, J. Org. Chem. 79 (2014) 12018–12032;
(b) B. Skillinghaug, J. Rydfjord, J. Sävmarker, M. Larhed, Microwave heated continuous flow palladium(II)-catalyzed desulfitative synthesis of aryl ketones, Org. Process Res. Dev. 20 (2016) 2005–2011;
(c) M. Behrends, J. Sävmarker, P.J.R. Sjöberg, M. Larhed, Microwave-assisted palladium(II)-catalyzed synthesis of aryl ketones from aryl sulfinates and direct ESI-MS studies thereof, ACS Catal. 1 (2011) 1455–1459;
(d) J. Liu, X. Zhou, H. Rao, F. Xiao, C.J. Li, G.J. Deng, Direct synthesis of aryl ketones by palladium-catalyzed desulfinative addition of sodium sulfinates to nitriles, Chem. Eur J. 17 (2011) 7996–7999;
(e) H. Wang, Y. Li, R. Zhang, K. Jin, D. Zhao, C. Duan, Palladium-catalyzed desulfitative conjugate addition of aryl sulfinic acids and direct ESI-MS for mechanistic studies, J. Org. Chem. 77 (2012) 4849–4853.

[12] (a) G.E. Reid, R.A.J. O'Hair, M.L. Styles, W.D. McFadyen, R.J. Simpson, Gas phase ion-molecule reactions in a modified ion trap: H/D exchange of non-covalent complexes and coordinatively unsaturated platinum complexes, Rapid Commun. Mass Spectrom. 12 (1998) 1701–1708;
(b) R. Vachet, Ion-molecule reactions as a probe of gas-phase structure of metal complexes, in: M.L. Gross, R. Caprioli (Eds.), in: N.M.M. Nibbering (Ed.), Fundamentals of and Applications to Organic (And Organometallic) Compounds, vol. 4, Elsevier, Amsterdam, 2005, pp. 629–638. The Encyclopedia of Mass Spectrometry;
(c) M.Y. Combariza, A.M. Fahey, A. Milshtey, R.W. Vachet, Gas-phase ion-molecule reactions of divalent metal complex ions: toward coordination structure analysis by mass spectrometry and some intrinsic coordination chemistry along the way, Int. J. Mass Spectrom. 244 (2005) 109–124.

[13] S. Wee, R.A.J. O'Hair, W.D. McFadyen, Gas phase ligand loss and ligand substitution reactions of platinum(II) complexes of tridentate nitrogen donor ligands, Rapid Commun. Mass Spectrom. 18 (2004) 1221–1226.

[14] (For studies on the use of formic acid to protonate coordinated ligands, see):
(a) G.N. Khairallah, R.A.J. O'Hair, Dehydrogenation of formic acid catalyzed by magnesium hydride anions, $HMgL_2$- (L = Cl and HCO_2), Int. J. Mass Spectrom. 254 (2006) 145–151;
(b) A. Zavras, G.N. Khairallah, M. Krstić, M. Girod, S. Daly, R. Antoine, P. Maitre, R.J. Mulder, S.A. Alexander, V. Bonačić-Koutecký, P. Dugourd, R.A.J. O'Hair, Ligand-induced substrate steering and reshaping of $[Ag_2(H)]^+$ scaffold for selective CO_2 extrusion from formic acid, Nat. Commun. 7 (2016) 11746;
(c) A. Zavras, M. Krstić, P. Dugourd, V. Bonačić-Koutecký, R.A.J. O'Hair, Selectivity effects in bimetallic catalysis: role of the metal sites in the decomposition of formic acid into H_2 and CO_2 by the coinage metal binuclear complexes [dppmMM'(H)]$^+$, ChemCatChem 9 (2017) 1298–1302;
(d) M. Krstić, Q. Jin, G.N. Khairallah, R.A.J. O'Hair, V. Bonačić-Koutecký, How to translate the $[LCu_2(H)]^+$ catalysed selective decomposition of formic acid into H_2 and CO_2 from the gas-phase into a zeolite, ChemCatChem 10 (2018) 1173–1177.

[15] (a) W.A. Donald, C.J. McKenzie, R.A.J. O'Hair, C–H bond activation of methanol and ethanol by a high-spin $Fe^{IV}O$ biomimetic complex, Angew. Chem. Int. Ed. 50 (2011) 8379–8383;
(b) A.K.Y. Lam, C. Li, G.N. Khairallah, B.B. Kirk, S.J. Blanksby, A.J. Trevitt, U. Wille, R.A.J. O'Hair, G. da Silva, Gas-phase reactions of aryl radicals with 2-butyne: an experimental and theoretical investigation employing the *N*-methyl-pyridinium-4-yl radical cation, Phys. Chem. Chem. Phys. 14 (2012) 2417–2426.

[16] W.A. Donald, G.N. Khairallah, R.A.J. O'Hair, The effective temperature of ions stored in a linear quadrupole ion trap mass spectrometer, J. Am. Soc. Mass Spectrom. 24 (2013) 811–815.

[17] (a) K.F. Lim, Program COLRATE. QCPE 643: calculation of gas-kinetic collision rate coefficients, QCPE Bull. 14 (3) (1994);
(b) T. Su, M.T. Bowers, Ion-Polar molecule collisions: the effect of ion size on ion-polar molecule rate constants; the parameterization of the average-dipole-orientation theory, Int. J. Mass Spectrom. Ion Phys. 12 (1973) 347–356.

[18] (a) Gaussian 09, revision a. 02 M.J. Frisch, G.W. Trucks, H.B. Schlegel, G.E. Scuseria, M.A. Robb, J.R. Cheeseman, G. Scalmani, V. Barone, G.A. Petersson, H. Nakatsuji, X. Li, M. Caricato, A.V. Marenich, J. Bloino, B.G. Janesko, R. Gomperts, B. Mennucci, H.P. Hratchian, J.V. Ortiz, A.F. Izmaylov, J.L. Sonnenberg, D. Williams-Young, F. Ding, F. Lipparini, F. Egidi, J. Goings, B. Peng, A. Petrone, T. Henderson, D. Ranasinghe, V.G. Zakrzewski, J. Gao, N. Rega, G. Zheng, W. Liang, M. Hada, M. Ehara, K. Toyota, R. Fukuda, J. Hasegawa, M. Ishida, T. Nakajima, Y. Honda, O. Kitao, H. Nakai, T. Vreven, K. Throssell, J.A. Montgomery Jr., J.E. Peralta, F. Ogliaro, M.J. Bearpark, J.J. Heyd, E.N. Brothers, K.N. Kudin, V.N. Staroverov, T.A. Keith, R. Kobayashi, J. Normand, K. Raghavachari, A.P. Rendell, J.C. Burant, S.S. Iyengar, J. Tomasi, M. Cossi, J.M. Millam, M. Klene, C. Adamo, R. Cammi, J.W. Ochterski, R.L. Martin, K. Morokuma, O. Farkas, J.B. Foresman, D.J. Fox, Gaussian, Inc., Wallingford CT, 2016;
(b) R. Dennington, T. Keith, J. Millam, GaussView, Version 5, Semichem Inc., Shawnee Mission, KS, 2009.

[19] Y. Zhao, D.G. Truhlar, The M06 suite of density functionals for main group

thermochemistry, thermochemical kinetics, noncovalent interactions, excited states, and transition elements: two new functionals and systematic testing of four M06-class functionals and 12 other functionals, Theor. Chem. Acc. 120 (2008) 215–241.
[20] G.A. Petersson, M.A. Al-Laham, A complete basis set model chemistry. II. Open-shell systems and the total energies of the first-row atoms, J. Chem. Phys. 94 (1991) 6081–6090.
[21] T. Clark, J. Chandrasekhar, G.W. Spitznagel, P.V.R. Schleyer, Efficient diffuse function-augmented basis sets for anion calculations. III. The 3-21+ G basis set for first-row elements, Li–F, J. Comput. Chem. 4 (1983) 294–301.
[22] B. Butschke, H. Schwarz, Mechanistic study on the gas-phase generation of "Rollover"-Cyclometalated $[M(bipy - H)]^+$ (M = Ni, Pd, Pt), Organometallics 29 (2010) 6002–6011.
[23] F. Weigend, F. Furche, R. Ahlrichs, Gaussian basis sets of quadruple zeta valence quality for atoms H–Kr, J. Chem. Phys. 119 (2003) 12753–12762.
[24] H.S. Yu, X. He, S.L. Li, D.G. Truhlar, MN15: a Kohn–Sham global-hybrid exchange–correlation density functional with broad accuracy for multi-reference and single-reference systems and noncovalent interactions, Chem. Sci. 8 (2016) 5032–5051.
[25] J.-D. Chai, M. Head-Gordon, Systematic optimization of long-range corrected hybrid density functionals, J. Chem. Phys. 128 (2008), 084106.
[26] (a) A.D. Becke, Density-functional exchange-energy approximation with correct asymptotic behaviour, Phys. Rev. 38 (1988) 3098;
(b) C. Lee, W. Yang, R.G. Parr, Development of the Colle-Salvetti correlation-energy formula into a functional of the electron density, Phys. Rev. B 37 (1988) 785;
(c) A.D. Becke, Density-functional thermochemistry. III. The role of exact exchange, J. Chem. Phys. 98 (1993) 5648–5652;
(d) F.J. Devlin, C.F.N. Chabalowski, M.J. Frisch, Ab initio calculation of vibrational absorption and circular dichroism spectra using density functional force fields, J. Chem. Phys. 98 (1994) 11623–11627;
(e) P.J. Stephens, T. Yanai, D.P. Tew, N.C. Handy, A new hybrid exchange–correlation functional using the Coulomb-attenuating method (CAM-B3LYP), Chem. Phys. Lett. 393 (2004) 51–57.
[27] S.A. McLuckey, D.E. Goeringer, Slow heating methods in tandem mass spectrometry, J. Mass Spectrom. 32 (1997) 461–474.
[28] P.D. Dau, P.B. Armentrout, M.C. Michelini, J.K. Gibson, Activation of carbon dioxide by a terminal uranium–nitrogen bond in the gas-phase: a demonstration of the principle of microscopic reversibility, Phys. Chem. Chem. Phys. 18 (2016) 7334–7340.
[29] (a) B. Milani, A. Marson, E. Zangrando, G. Mestroni, J. Meine Ernsting, C.J. Elsevier, New monocationic methylpalladium(II) compounds with several bidentate nitrogen-donor ligands: synthesis, characterisation and reactivity with CO, Inorg. Chim. Acta. 327 (2002) 188–201;
(b) B. Milani, G. Corso, E. Zangrando, L. Randaccio, G. Mestroni, Crystal structure and dynamic behavior of a new class of monocationic organometallic PdII compounds with two molecules of bidentate ligands: $[Pd(L–L)(N–N)(CH_2NO_2)][PF_6]$ (L–L = N–N, dppp), Eur. J. Inorg. Chem. 11 (1999) 2085–2093;
(c) R. Garrone, A.M. Romano, R. Santi, R. Millini, Synthesis, structure, and reactivity of the novel pentacoordinate palladium complex $[Pd(Phen)_2(-CO_2CH_3)](PF_6)$, Organometallics 17 (1998) 4519–4522.
[30] M.L. Parker, S. Gronert, Investigating reduced metal species via sequential ion/ion and ion/molecule reactions: the reactions of transition metal phenanthrolines with allyl iodide, Int. J. Mass Spectrom. 418 (2017) 73–78.
[31] For a review on three-coordinate Pt(II) complexes, see: M.A. Ortuño, S. Conejero, A. Lledós, True and masked three-coordinate T-shaped platinum(II) intermediates Beilstein J. Org. Chem. 9 (2013) 1352.
[32] J.E. Bartmess "Negative ion energetics data" in NIST Chemistry WebBook, NIST Standard Reference Database Number 69, Eds. P.J. Linstrom and W.G. Mallard, last accessed 28 September 2018.